Original

Short, R.; Carta, M.; Grazia Bezzu, C.; Fritsch, D.; Kariuki, B.M.;
McKeown, N.B.:

Hexaphenylbenzene-based polymers of intrinsic microporosity

In: Chemical Communications : ChemComm (2011) RSC Publishing

DOI: 10.1039/c1cc11717c

ChemComm

Cite this: *Chem. Commun.*, 2011, **47**, 6822–6824

www.rsc.org/chemcomm

COMMUNICATION

Hexaphenylbenzene-based polymers of intrinsic microporosity†

Rhys Short,[a] Mariolino Carta,[a] C. Grazia Bezzu,[a] Detlev Fritsch,[b] Benson M. Kariuki[a] and Neil B. McKeown*[a]

Received 25th March 2011, Accepted 20th April 2011
DOI: 10.1039/c1cc11717c

Microporous polymers derived from the 1,2- and 1,4-regioisomers of di(3′,4′-dihydroxyphenyl)tetraphenylbenzene have very different properties with the former being composed predominantly of cyclic oligomers whereas the latter is of high molar mass suitable for the formation of robust solvent-cast films of high gas permeability.

Hexaphenylbenzene (HPB) is an interesting structural unit for the construction of organic materials due to its rigidity and propeller-like shape, which arise from the mutual steric interactions of the phenyl groups. Derivatives of HPB have been of considerable interest for a wide variety of applications in materials chemistry including their use as organic electronic materials,[1,2] as precursors to synthetic graphene fragments,[3] as rigid structural building units for crystal engineering[4–9] and liquid crystals,[10] as components for photo-induced electron transfer systems,[11–13] for the site-isolation of reactive species,[14] and as proton-transport materials.[15,16] They have also been used extensively for making polymers with high glass-transition temperatures.[17]

The shape of HPB with its many shallow concavities leads to imperfect packing in the solid state as illustrated by the numerous examples of inclusion crystal structures of its derivatives.[4–9] This feature, often termed 'internal molecular free volume',[18] is a prerequisite for the formation of macromolecular structures that pack inefficiently in the solid state.[19] Therefore, it was anticipated that HPB would be a successful component for making novel Polymers of Intrinsic Microporosity (HPB-PIMs) with different properties to those prepared previously from spirobisindane[20–23] or triptycene-based components.[24,25]

For PIMs, the microporosity arises from their fused-ring structure, which prevents conformational rearrangement of the contorted shape of the macromolecule. An efficient polymerisation reaction that provides a fused-ring linking group is the double aromatic nucleophilic substitution reaction between monomers that contain catechol (*i.e.* 1,2-dihydroxyphenyl) and 1,2-difluoroaryl units. For the latter, the commercially available and highly reactive 2,3,5,6-tetrafluoroterephthalonitrile is particularly convenient. Hence, to prepare a HPB-PIM, one of the three possible regioisomers of di-(3′,4′-dihydroxyphenyl)-tetraphenylbenzene, which arise from the *ortho*- (1,2-), *meta*- (1,3-) or *para*- (1,4-) substitution of the catechol units on the central benzene ring, is required. This communication reports on the very different properties of the HPB-PIMs derived from 1,2- and 1,4-di(3′,4′-dihydroxyphenyl)tetraphenylbenzene, **1** and **2**, respectively.

The syntheses of monomers **1** and **2** and of the polymers **HPB-PIM-1** and **HPB-PIM-2** derived from them is outlined in Scheme 1. The key step involves the well-established Diels–Alder reaction between appropriately substituted diphenylacetylenes and tetraphenylcyclopentadienones.[17] Attempts to prepare monomer **1** *via* the reaction between di(3,4-dimethoxyphenyl)acetylene and tetraphenylcyclopentadienone failed. Monomer **2** was prepared regioselectively with no apparent contamination of the 1,3-isomer.†

Both **HPB-PIM-1** and **HPB-PIM-2** proved readily soluble in a range of organic solvents including THF and $CHCl_3$ but only the latter could be purified by the removal of oligomeric material by reprecipitation from the slow addition of the polymer solution into a non-solvent such as methanol or acetone. Analysis of crude **HPB-PIM-1** by Gel Permeation Chromatography (GPC) indicates a distinctly bimodal mass distribution with a minor fraction corresponding to a mass range of 20 000–40 000 mol g^{-1} and the major fraction to a range of only 1000–5000 mol g^{-1} relative to polystyrene standards. Matrix Assisted Laser Desorption Ionisation Mass Spectrometry (MALDI-MS) shows the presence of cyclic oligomers (n = 2–8; *i.e.* [2 + 2], [3 + 3],. . .[8 + 8]). On monitoring the progress of the polymerization by thin layer chromatography, a distinct yellow spot at relatively low polarity (R_f 0.8; ethyl acetate/hexane 8 : 2) was observed. Isolation of this material in up to 15% overall yield was achieved by column chromatography and MALDI-MS confirmed it to be the [2 + 2] cyclic oligomer **3** (Fig. 1). Single crystal X-ray diffraction (XRD) revealed that the dibenzodioxane rings within this cyclic oligomer deviate from planarity.[26] All of the crystal structures held within the Cambridge Structural Database (CSD) of compounds that contain dibenzodioxane demonstrate the strong tendency of this structural unit to be planar. For cyclic oligomer **3** this distortion from planarity must be attributed to significant ring strain originating from the structure and rigidity of the TPB units. Investigation of the

[a] *School of Chemistry, Cardiff University, Cardiff, CF10 3AT, UK. E-mail: mckeownnb@cardiff.ac.uk; Tel: 44 2920 875850*
[b] *Institute of Materials Research, Helmholtz-Zentrum Geesthacht, Max-Planck-Str. 1, 21502 Geesthacht, Germany*

† Electronic supplementary information (ESI) available: Synthetic procedures and physical methodology. CCDC 819213. For ESI and crystallographic data in CIF or other electronic format see DOI: 10.1039/c1cc11717c

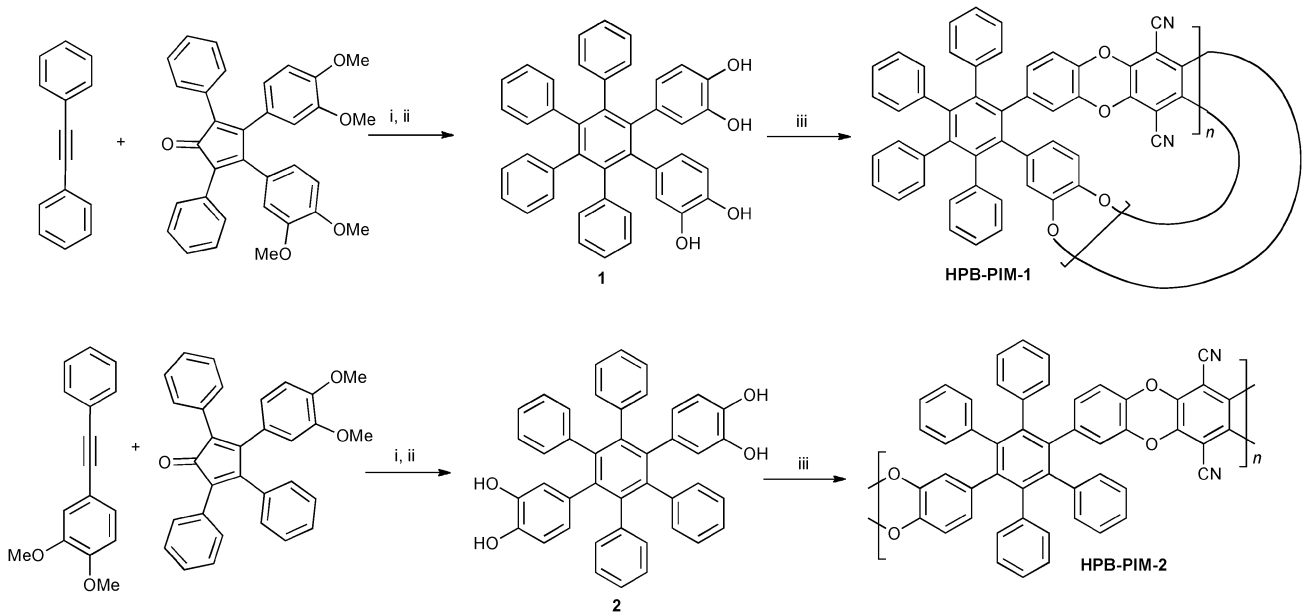

Scheme 1 *Reagents and conditions*: (i) diphenyl ether, 250 °C; (ii) BBr_3, DCM, 20 °C, 1 h; (iii) 2,3,5,6-tetrafluoroterephthalonitrile, DMF, K_2CO_3, 65 °C, 96 h.

packing within the crystal structure reveals wide, solvent-filled channels which run along the crystal *z*-axis. Desolvation of these crystals occurs very rapidly to give an amorphous powder, which demonstrates significant nitrogen (N_2) adsorption at 77 K. An apparent BET surface area of 162 $m^2\ g^{-1}$ is calculated from the N_2 adsorption isotherm (Fig. 2). Although the observed microporosity for the amorphous powder of **3** cannot be directly linked to the crystal structure, the large quantity of included solvent within these channels demonstrates the inefficient molecular packing that leads to intrinsic microporosity. Crude **HPB-PIM-1** demonstrates a larger apparent BET surface area of 425 $m^2\ g^{-1}$ (Fig. 2).

In contrast, GPC analysis of **HPB-PIM-2**, purified by reprecipitation, indicates a relatively high molecular mass (M_n = 40 000 and M_w = 106 000 g mol^{-1}). In addition, no cyclic oligomers were apparent from MALDI-MS analysis as might expected from the 1,4-arrangement of the catechol moieties on the central benzene ring of the TPB unit of monomer **2**, which would inhibit macrocycle formation. The microporosity of **HPB-PIM-2** also proved significantly greater than that of **HPB-PIM-1** with an apparent BET surface area of 527 $m^2\ g^{-1}$ calculated from its N_2 adsorption isotherm (Fig. 2). A particularly attractive property of **HPB-PIM-2** arising from its high average molecular mass is its ability to form robust, optically clear self-standing films by simple casting from a dilute solution of the polymer in $CHCl_3$. The availability of robust, defect-free films facilitates the measurement of gas permeability using time-lag methodology. The permeability, diffusivity and solubility coefficients for O_2, N_2, He, H_2, CO_2 and CH_4 are presented in Table 1. In common with other highly permeable glassy polymers the order of permeability is $CO_2 > H_2 > He > O_2 > CH_4 > N_2$ which reflects the contribution of both solubility and diffusivity to the gas permeability.[27]

Table 1 Permeability data for **HPB-PIM-2**. The corresponding data for PIM-1 is also given for N_2 and CO_2[28]

	Diffusivity ($cm^2\ s^{-1} \times 10^8$)	Solubility (cm^3(STP)/$cm^3\ cmHg \times 10^3$)	Permeability (Barrer)	Perm.-Selectivity PX/PN_2
O_2	93.5	23	217	3.3
N_2 (PIM-1)	34.8 (160)	19 (37)	66.5 (610)	1 (1)
He	3100	1.1	340	5.1
H_2	1700	4.3	723	10.9
CO_2 (PIM-1)	46.2 (160)	375 (700)	1730 (11300)	26.1 (18.5)
CH_4	14.0	87	122	1.8

PIM-1, derived from the reaction between 5,5′,6,6′-tetrahydroxy-3,3,3′,3′-tetramethyl-1,1′-spirobisindane and 2,3,5,6-tetrafluoroterephthalonitrile, provides permeability data that represent an excellent compromise in the trade-off between the desirable properties of high permeability and good selectivity required for efficient gas separation membranes.[27,28] The data for **HPB-PIM-2** show significantly lower permeabilities relative to PIM-1 but enhanced selectivities (*e.g.* selectivity for CO_2 *vs.* N_2 = 26). The reduced permeability relative to PIM-1 can be attributed both to lower diffusivity due to lower intrinsic microporosity and lower solubility due to a smaller concentration of polar groups (*i.e.* ether and nitrile). Despite its relatively modest performance relative to PIM-1, **HPB-PIM-2** still demonstrates permeabilities that are attractive for gas separation membranes and may possess other properties that provide advantages for this application (*e.g.* reduced physical ageing effects due to greater chain rigidity). Simple chemical modifications to introduce greater polarity into the polymer may also provide enhancement of gas separation properties and such studies are planned. The highly fluorescent nature of these polymers also suggest utility as the active material in optical sensors[29] and work related to this is on-going.

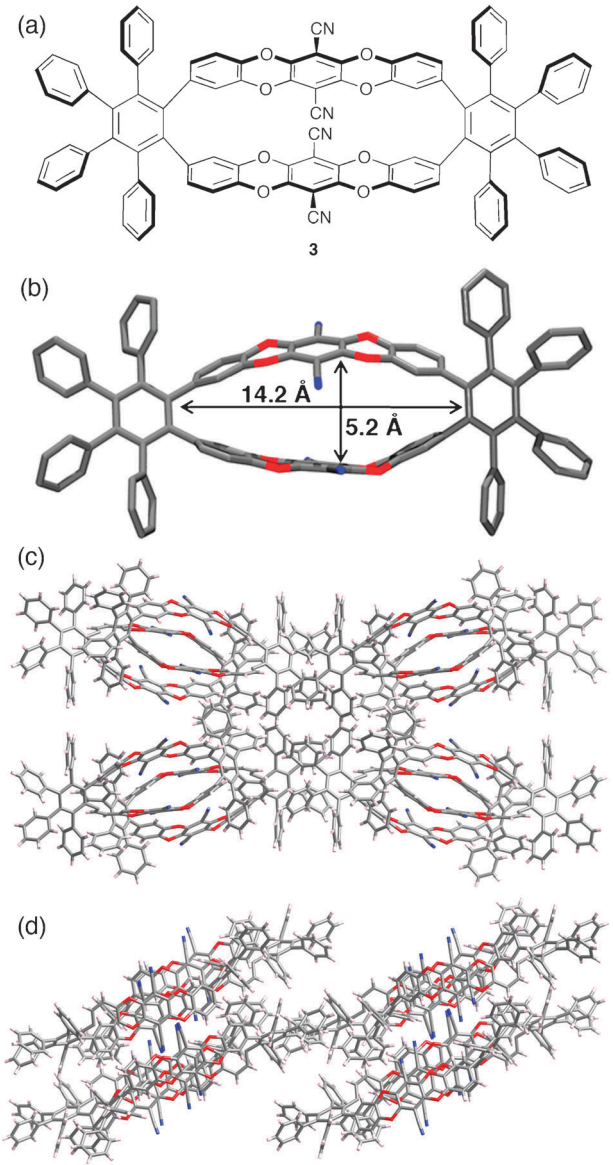

Fig. 1 (a) The molecular structure of **3** and (b) its structure from a single crystal X-ray diffraction study. The packing of **3** viewed along (c) the *z*-axis and (d) the *y*-axis of the crystal showing the channels that are filled with disordered solvent.

We acknowledge funding from EPSRC grants EP/G01244X (MC) and EP/H024034/1 (CGB).

Notes and references

1 S. Watanabe and J. Kido, *Chem. Lett.*, 2007, **36**, 590–591.
2 Z. Li, S. Ye, Y. Liu, G. Yu, W. Wu, J. Qin and Z. Li, *J. Phys. Chem. B*, 2010, **114**, 9101–9108.
3 W. Pisula, X. L. Feng and K. Müllen, *Chem. Mater.*, 2011, **23**, 554–567.
4 K. Kobayashi, T. Shirasaka, A. Sato, E. Horn and N. Furukawa, *Angew. Chem., Int. Ed.*, 1999, **38**, 3483–3486.
5 K. Kobayashi, A. Sato, S. Sakamoto and K. Yamaguchi, *J. Am. Chem. Soc.*, 2003, **125**, 3035–3045.
6 K. Kobayashi, N. Kobayashi, M. Ikuta, B. Therrien, S. Sakamoto and K. Yamaguchi, *J. Org. Chem.*, 2005, **70**, 749–752.
7 K. E. Maly, E. Gagnon, T. Maris and J. D. Wuest, *J. Am. Chem. Soc.*, 2007, **129**, 4306–4322.

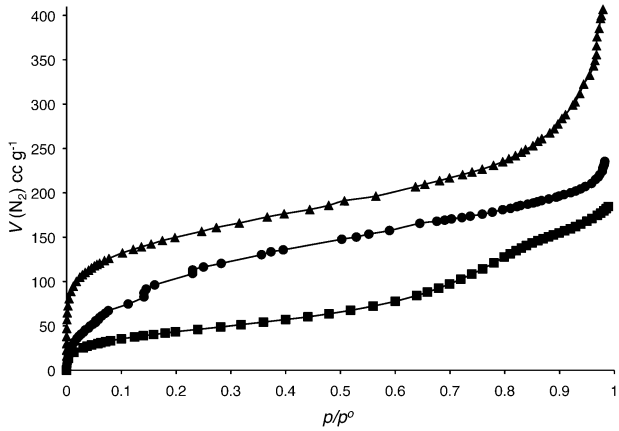

Fig. 2 Nitrogen adsorption isotherms for **3** (■); **HPB-PIM-1** (●) and **HPB-PIM-2** (▲).

8 E. Gagnon, S. D. Halperin, V. Metivaud, K. E. Maly and J. D. Wuest, *J. Org. Chem.*, 2010, **75**, 399–406.
9 E. Gagnon, T. Maris, P.-M. Arseneault, K. E. Maly and J. D. Wuest, *Cryst. Growth Des.*, 2010, **10**, 648–657.
10 Y. H. Geng, A. Fechtenkotter and K. Müllen, *J. Mater. Chem.*, 2001, **11**, 1634–1641.
11 R. Rathore, C. L. Burns and S. A. Abdelwahed, *Org. Lett.*, 2004, **6**, 1689–1692.
12 D. L. Sun, S. V. Rosokha and J. K. Kochi, *Angew. Chem., Int. Ed.*, 2005, **44**, 5133–5136.
13 G. Kodis, Y. Terazono, P. A. Liddell, J. Andreasson, V. Garg, M. Hambourger, T. A. Moore, A. L. Moore and D. Gust, *J. Am. Chem. Soc.*, 2006, **128**, 1818–1827.
14 R. Rathore, C. L. Burns and I. A. Guzei, *J. Org. Chem.*, 2004, **69**, 1524–1530.
15 L. Jimenez-Garcia, A. Kaltbeitzel, W. Pisula, J. S. Gutmann, M. Klapper and K. Müllen, *Angew. Chem., Int. Ed.*, 2009, **48**, 9951–9953.
16 S. Matsumura, A. R. Hlil, M. A. K. Al-Souz, J. Gaudet, D. Guay and A. S. Hay, *J. Polym. Sci., Part A: Polym. Chem.*, 2009, **47**, 5461–5473.
17 C. Kubel, S. L. Chen and K. Müllen, *Macromolecules*, 1998, **31**, 6014–6021.
18 T. M. Long and T. M. Swager, *Adv. Mater.*, 2001, **13**, 601–604.
19 N. B. McKeown and P. M. Budd, *Macromolecules*, 2010, **43**, 5163–5176.
20 P. M. Budd, E. S. Elabas, B. S. Ghanem, S. Makhseed, N. B. McKeown, K. J. Msayib, C. E. Tattershall and D. Wang, *Adv. Mater.*, 2004, **16**, 456–459.
21 P. M. Budd, B. S. Ghanem, S. Makhseed, N. B. McKeown, K. J. Msayib and C. E. Tattershall, *Chem. Commun.*, 2004, 230–231.
22 M. Carta, J. Msayib Kadhum, M. Budd Peter and B. McKeown Neil, *Org. Lett.*, 2008, **10**, 2641–2643.
23 P. M. Budd, B. Ghanem, K. Msayib, N. B. McKeown and C. Tattershall, *J. Mater. Chem.*, 2003, **13**, 2721–2726.
24 B. S. Ghanem, K. J. Msayib, N. B. McKeown, K. D. M. Harris, Z. Pan, P. M. Budd, A. Butler, J. Selbie, D. Book and A. Walton, *Chem. Commun.*, 2007, 67–69.
25 B. S. Ghanem, M. Hashem, K. D. M. Harris, K. J. Msayib, M. C. Xu, P. M. Budd, N. Chaukura, D. Book, S. Tedds, A. Walton and N. B. McKeown, *Macromolecules*, 2010, **43**, 5287–5294.
26 A. W. Cordes and C. K. Fair, *Acta Crystallogr., Sect. B: Struct. Crystallogr. Cryst. Chem.*, 1974, **30**(Pt. 6), 1621–1623.
27 P. M. Budd and N. B. McKeown, *Polym. Chem.*, 2010, **1**, 63–68.
28 P. M. Budd, N. B. McKeown, B. S. Ghanem, K. J. Msayib, D. Fritsch, L. Starannikova, N. Belov, O. Sanfirova, Y. Yampolskii and V. Shantarovich, *J. Membr. Sci.*, 2008, **325**, 851–860.
29 Y. Wang, N. B. McKeown, K. J. Msayib, G. A. Turnbull and I. D. W. Samuel, *Sensors*, 2011, **11**, 2478–2487.

